THE JOURNAL OF BIOLOGICAL CHEMISTRY VOL. 282, NO. 51, pp. 36905–36913, December 21, 2007

Novel Conantokins from *Conus parius* Venom Are Specific Antagonists of *N*-Methyl-D-aspartate Receptors*

Received for publication, August 9, 2007, and in revised form, October 17, 2007 Published, JBC Papers in Press, October 25, 2007, DOI 10.1074/jbc.M706611200

Russell W. Teichert[‡1], Elsie C. Jimenez[‡§], Vernon Twede[‡], Maren Watkins[¶], Michael Hollmann[‖], Grzegorz Bulaj[**], and Baldomero M. Olivera[‡]

From the Departments of [‡]Biology, [¶]Pathology, and [**]Medicinal Chemistry, University of Utah, Salt Lake City, Utah 84112, the [§]Department of Physical Sciences, College of Science, University of the Philippines Baguio, Baguio City 2600, Philippines, and the [‖]Department of Biochemistry I-Receptor Biochemistry, Faculty of Chemistry and Biochemistry, Ruhr University Bochum, D-44780 Bochum, Germany

We report the discovery and characterization of three conantokin peptides from the venom of *Conus parius*. Each peptide (conantokin-Pr1, -Pr2, and -Pr3) contains 19 amino acids with three γ-carboxyglutamate (Gla) residues, a post-translationally modified amino acid characteristic of conantokins. The new peptides contain several amino acid residues that differ from previous conantokin consensus sequences. Notably, the new conantokins lack Gla at the 3rd position from the N terminus, where the Gla residue is replaced by either aspartate or by another post-translationally modified residue, 4-*trans*-hydroxyproline. Conantokin-Pr3 is the first conantokin peptide to have three different post-translational modifications. Conantokins-Pr1 and -Pr2 adopt α-helical conformations in the presence of divalent cations (Mg^{2+} and Ca^{2+}) but are generally unstructured in the absence of divalent cations. Conantokin-Pr3 adopts an α-helical conformation even in the absence of divalent cations. Like other conantokins, the new peptides induced sleep in young mice and hyperactivity in older mice upon intracranial injection. Electrophysiological assays confirmed that conantokins-Pr1, -Pr2, and -Pr3 are *N*-methyl-D-aspartate (NMDA) receptor antagonists, with highest potency for NR2B-containing NMDA receptors. Conantokin-Pr3 demonstrated ~10-fold selectivity for NR2B-containing NMDA receptors. However, conantokin-Pr2 showed minimal differences in potency between NR2B and NR2D. Conantokins-Pr1, -Pr2, and -Pr3 all demonstrated high specificity of block for NMDA receptors, when tested against various ligand-gated ion channels. *Conus parius* conantokins allow for a better definition of structural and functional features of conantokins as ligands targeting NMDA receptors.

Most families of peptides extracted from the venoms of marine cone snails (genus *Conus*) are known as conotoxins; these peptides have an unusually high density of disulfide cross-links. In contrast, the conantokins, which are also *Conus* venom peptides, typically lack disulfide bonds but characteristically contain several residues of an unusual post-translationally modified amino acid, γ-carboxyglutamate (Gla).[2] Conantokins were first identified by their ability to cause sleep in young mice and hyperactivity in older mice when injected intracranially (1, 2). Subsequently, they were characterized as antagonists of the *N*-methyl-D-aspartate (NMDA) receptor class of ionotropic glutamate receptors (3–5). The first conantokin peptide purified from the venom of *Conus geographus*, conantokin-G (con-G), was reported over 20 years ago (1). However, in the ensuing decades only three additional conantokin peptides have been reported in the scientific literature as follows: conantokin-T (con-T) (3), conantokin-R (con-R) (6), and conantokin-L (con-L) (7); see Table 1 for a comparison of conantokin sequences.

The characterization of con-G demonstrated that it is a selective antagonist of NMDA receptors containing the NR2B subunit (8). This pharmacological selectivity has raised general interest in several potential clinical applications that include developing conantokin peptides as drugs for neuroprotection (*e.g.* after ischemic stroke) (9–11), pain (12–14), epilepsy (3, 6, 7, 15), and probing mechanisms of drug addiction (16). Con-G (CGX-1007, Cognetix, Inc.) has reached phase I clinical trials for both pain and epilepsy (14).

In this work, we have identified three peptides that belong to the conantokin family from the venom of the Indo-Pacific fish-hunting cone snail species, *Conus parius*. We report the purification, synthesis, and characterization of these conantokin peptides. In all previous cases, only a single conantokin peptide was purified and characterized from the venom of any particular *Conus* species. The characterization of these novel peptides significantly expands the body of knowledge regarding the conantokin family. The *C. parius* conantokins contain several amino acids that vary from consensus sequences of previously characterized conantokins, including novel post-translational modifications. Consequently, these peptides allow us to better define significant biochemical features of conantokins for targeting NMDA receptors.

* This work was supported by NiGM Program Project Grant GM48677 from National Institutes of Health. The costs of publication of this article were defrayed in part by the payment of page charges. This article must therefore be hereby marked "*advertisement*" in accordance with 18 U.S.C. Section 1734 solely to indicate this fact.

[1] To whom correspondence should be addressed: 257 S. 1400 E., Salt Lake City, UT 84112-0840. Tel.: 801-581-8370; Fax: 801-585-5010; E-mail: russ_teichert@yahoo.com.

[2] The abbreviations used are: Gla, γ,γ-carboxyglutamate; ACN, acetonitrile; con, conantokin; Hyp, *O*,4-*trans*-hydroxyproline; MALDI, matrix-assisted laser desorption ionization; NMDA, *N*-methyl-D-aspartate; HPLC, high performance liquid chromatography; nAChR, nicotinic acetylcholine receptor.

EXPERIMENTAL PROCEDURES

Preparation of Venom Extract—Venom ducts of *C. parius* were dissected from the cone snails as described previously (17). The collected venom ducts were lyophilized and stored at −80 °C. Fifteen lyophilized venom ducts were ground over liquid nitrogen with mortar and pestle. Venom was extracted sequentially with 5 ml of H_2O, 3 ml each of 20% acetonitrile (ACN), 40% ACN, and 60% ACN. The venom suspension was sonicated in the extracting solvent five times in 30-s intervals at 0 °C and then centrifuged at 5000 × *g* for 5 min. The combined supernatant (crude venom extract) was lyophilized and stored at −20 °C until further purification.

Peptide Purification—The crude venom extract was resuspended in a mixture of 0.1% trifluoroacetic acid (solvent A) and 0.085% trifluoroacetic acid in 90% ACN (solvent B) and applied into a Vydac C_{18} analytical column (4.6 × 250 mm, 5 μm particle size). Peptides were eluted with a gradient of ACN using solvents A and B. The effluents were monitored at 220 nm. Individual peptides from various peaks were further purified by analytical HPLC runs. Each peptide solution was lyophilized and stored at −20 °C.

Peptide Sequencing—One nmol of each of the purified peptides was separately dissolved in 500 μl of a mixture of 80% solvent A and 20% solvent B. The pH was adjusted to 7.5 with 0.5 M Tris base, and dithiothreitol was then added to a final concentration of 10 mM. The solution was flushed with argon, incubated for 20 min at 65 °C, and cooled to room temperature. Two microliters of 4-vinylpyridine were added to the solution, which was placed in the dark at room temperature for 25 min. The peptide solution was then diluted with 500 μl of solvent A and applied into a C_{18} analytical column. The purified alkylated peptide was sequenced by automated Edman degradation (18) on an Applied Biosystem model 492 sequenator, courtesy of Dr. Robert Schackmann of the DNA/Peptide Facility, University of Utah. The phenylthiohydantoin-derivatives were purified by analytical HPLC.

Peptide Synthesis—Based on peptide sequences, three peptides were identified as conantokins. The conantokin peptides were synthesized using standard *N*-(9-fluorenyl)methoxycarbonyl (Fmoc)-protected amino acids in an ABI model 430A peptide synthesizer, courtesy of Dr. Scott Endicott of the DNA/Peptide Facility, University of Utah. After synthesis, each peptide was cleaved from 20 mg of resin by treatment with 1 ml of a mixture of trifluoroacetic acid/H_2O/1,2-ethanedithiol/phenol/thioanisole (82.5/5/2.5/5/5 by volume) with agitation for 1 h at room temperature. The mixture was filtered under vacuum into methyl-*tert*-butyl ether at −10 °C. Linear peptide was collected by centrifugation at 5000 × *g* for 5 min, washed with methyl-*tert*-butyl ether, and centrifuged again. The pellet was dissolved in 20% ACN in 0.1% trifluoroacetic acid and applied into a Vydac C_{18} semi-preparative column (10 × 250 mm, 5-μm particle size). Elution was carried out at 5 ml/min using a gradient of solvent B.

Mass Spectrometry—Matrix-assisted laser desorption ionization (MALDI) mass spectra were obtained using a Voyager GE STR mass spectrometer at the Mass Spectrometry and Proteomic Core Facility of the University of Utah.

Molecular Cloning—cDNA was prepared by reverse transcription of RNA isolated from a *C. parius* venom duct as described previously (19). This cDNA was used as a template for PCR with oligonucleotides corresponding to the conserved signal sequence and 3′-untranslated region sequences of conantokin prepropeptides. The resulting PCR products were purified using the high pure PCR product purification kit (Roche Diagnostics) following the manufacturer's suggested protocol. The eluted DNA fragments were annealed to pAMP1 vector, and the resulting products were transformed into competent DH5α cells, using the CloneAmp pAMP system for rapid cloning of amplification products (Invitrogen) following the manufacturer's suggested protocols. The nucleic acid sequences of the resulting conantokin encoding clones were determined according to the standard protocol for automated sequencing.

Bioassay—Mice were injected intracranially with 20 μl of peptide in normal saline solution using a syringe with 29-gauge needle according to the method described earlier (20). Mice injected intracranially with an equal volume of normal saline solution served as negative controls. After injection, the mice were placed in cages for observation.

Circular Dichroism Spectroscopy—CD data were collected on an Aviv 62DS circular dichroism spectropolarimeter (instrument belonging to Dr. Michael Kay, University of Utah). All measurements were taken at room temperature in a 0.1-cm path length cuvette between 200 and 250 nm. Peptides were dissolved at 90 μM final concentration in 10 mM sodium phosphate buffer, pH 7.0, with or without 2 mM $MgCl_2$. Peptides were separately dissolved at 90 μM final concentration in 10 mM HEPES buffer, pH 7.0, with or without 2 mM $CaCl_2$. The molar ellipticity (θ) was calculated by using the following equation: $\theta = (100 \times (\text{CD signal at } 222 \text{ nm}))/((n-1) \times L \times (\text{concentration of peptide in mM}))$, where n = number of residues in the peptide; L = pathlength of the cuvette in cm; and the CD signal is in millidegrees. The CD signal was adjusted by subtracting the CD signal for buffer solution alone from the CD signal for the solution containing peptide. Molar ellipticity of −40,000 degrees cm^2 $dmol^{-1}$ was estimated to be a perfect α-helix (100% α-helix). The percent helical conformation was calculated by assuming a linear relationship in comparison with 100% α-helix.

Heterologous Expression of Receptors in Xenopus Oocytes—The rat NMDA receptor clones used were NR1–3b, NR2A, NR2B, NR2C, and NR2D (GenBank™ accession numbers U08266, AF001423, U11419, U08259, and U08260, respectively). Dr. Steven M. Sine, Mayo Clinic College of Medicine, provided the mouse muscle nAChR clones in the cytomegalovirus-based pRBG4 vector. Dr. Stephen F. Heinemann, The Salk Institute, provided rat neuronal nAChR clones. Human neuronal nAChR clones were provided by Dr. Jim Garrett, Cognetix, Inc. α-Amino-3-hydroxy-5-methyl-4-isoxazole propionate receptor clones were provided by Dr. Erin Meyer and Dr. A. Villu Maricq, University of Utah.

With the exception of GluR3 and the mouse muscle nAChR clones, all of the expression clones were used to make capped RNA for injection into the oocytes of *Xenopus laevis* frogs (most clones expressed genes from a T7 promoter). The har-

vesting of *Xenopus* oocytes was described previously in detail (21). Capped RNA was prepared using *in vitro* RNA transcription kits from Ambion, Inc., according to the manufacturer's protocols. For expression of NMDA receptors and neuronal nAChRs, typically 5 ng of each subunit capped RNA was injected per oocyte. For expression of skeletal muscle nAChRs and GluR3, 1 ng of each subunit cDNA was injected into the nucleus of each oocyte. The plasmid constructs encoding mouse muscle nAChR subunits and GluR3 contain genes expressed from a cytomegalovirus promoter. Oocyte recordings were obtained 1–6 days post-injection.

Electrophysiology—Voltage clamp recording of *Xenopus* oocytes was conducted as described in detail previously (21). Briefly, all oocytes were voltage-clamped at −70 mV. Oocytes expressing NMDA receptors were gravity perfused with Mg^{2+}-free ND96 buffer (96.0 mM NaCl, 2.0 mM KCl, 1.8 mM $CaCl_2$, 5 mM HEPES, pH 7.2–7.5). $MgCl_2$ was not included in ND96 buffer used for testing NMDA receptors because Mg^{2+} blocks NMDA receptors. For all other electrophysiological tests, oocytes were gravity perfused with ND96 buffer (96.0 mM NaCl, 2.0 mM KCl, 1.8 mM $CaCl_2$, 1 mM $MgCl_2$, 5 mM HEPES, pH 7.2–7.5). In all cases, bovine serum albumin was added to buffer at a final concentration of 0.1 mg/ml to reduce nonspecific adsorption of peptide. Currents were elicited by 1-s pulses of gravity-perfused agonist solution once per min or once per 2 min, depending on the receptor recovery from desensitization. 200 μM glutamate and 20 μM glycine were used as co-agonists for NMDA receptors; 10–200 μM acetylcholine was employed as the agonist for the various nAChRs. Buffer was perfused continuously over the oocytes between agonist pulses, with the exception of 5–10-min equilibration periods, during which buffer flow was halted for the application of a peptide to an oocyte in a static bath. To identify the effect of a peptide on the receptor heterologously expressed in an oocyte, the amplitude of the elicited current following the peptide application and equilibration period was calculated as a percentage of the amplitude of the elicited current prior to toxin application. All data recordings were conducted at room temperature. Data acquisition was automated by a virtual instrument made by Doju Yoshikami of the University of Utah. Concentration-response curves were generated using Prism software (GraphPad Software, Inc.), with the following equation, where *n*H is the Hill coefficient and IC_{50} is the concentration of peptide causing half-maximal block: % response = $100/\{1 + ([\text{peptide}]/IC_{50})^{nH}\}$.

RESULTS

Purification of Conantokins from C. parius Venom—One strategy employed for identifying the molecular targets of *Conus* peptides has been to assess HPLC-separated fractions from crude venom extracts for biological activity using a behavioral assay on mice. This approach allowed us to isolate three peptides from a single venom preparation of *C. parius* that all induced sleep in 10-day-old mice when injected intracranially. Using reverse-phase HPLC, the crude venom extract gave the elution profile shown in Fig. 1*A*. Three peaks containing the sleep-inducing activities were further fractionated to homogeneity as shown in Fig. 1, *B–K*, giving rise to three distinct peptides described below.

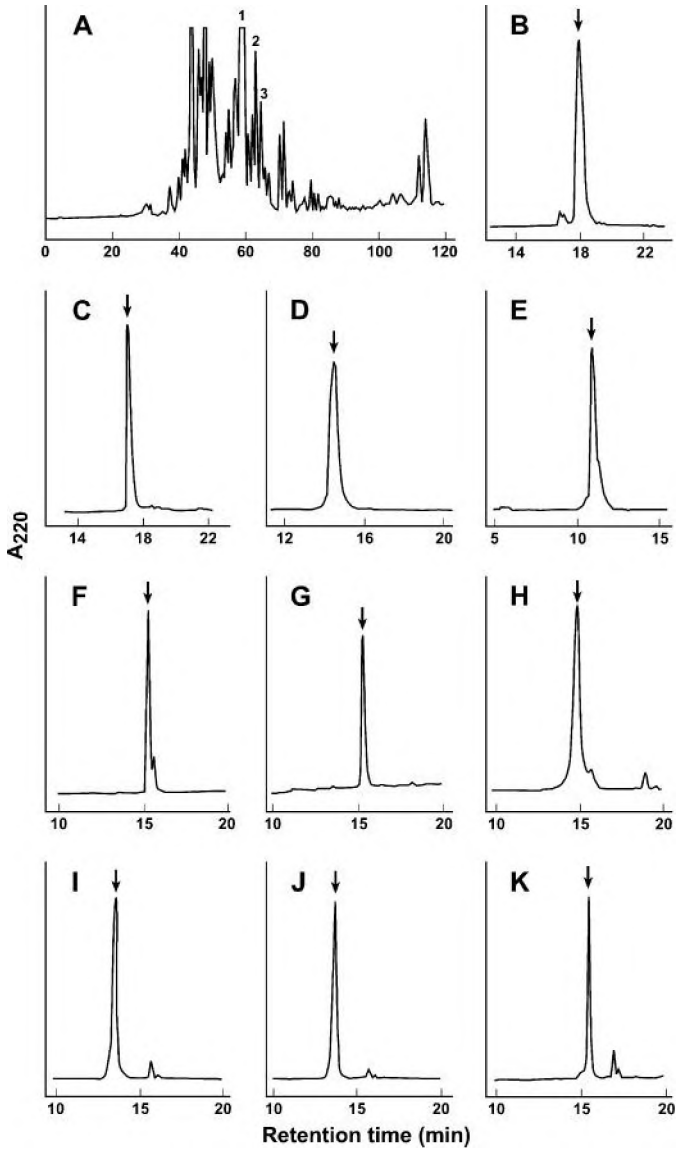

FIGURE 1. **Purification of conantokins.** A C_{18} HPLC analytical column was used in each purification step with a gradient of solvent B using 0.1% trifluoroacetic acid (solvent A) and 0.085% trifluoroacetic acid in 90% ACN (solvent B). The flow rate was 1 ml/min in each step. The *arrow* indicates the fraction containing the peptide. *A*, fractionation of *C. parius* crude venom extract prepared as described under "Experimental Procedures" at 0–60% solvent B for 120 min. *B* and *C*, purification of con-Pr1 from peak 1 in solvent A at 20–45% solvent B over 25 min in each step. *D–G*, purification of con-Pr2 from peak 2 in solvent A at 25–50% solvent B for 25 min, 25–75% solvent B for 20 min, 20–70% solvent B for 20 min, and 20–70% solvent B for 20 min, respectively. *H–K*, purification of con-Pr3 from peak 3 in solvent A at 25–45% solvent B for 20 min, 25–65% solvent B for 20 min, 25–65% solvent B for 20 min, and 20–70% solvent B for 20 min, respectively.

Each of the purified peptides was reduced, alkylated, and sequenced as described under "Experimental Procedures" by Edman chemical analysis. MALDI mass spectrometry was used to confirm the masses, which showed masses that differed by 44 mass units for the three peptides, indicating the presence of Gla residues.

In Fig. 1*C*, the purified peptide has 19 amino acid residues with the sequence GEDγYAγGIRγYQLIHGKI∧ where γ indicates Gla and the ∧ indicates free acid C terminus. MALDI mass spectrometry of the peptide gave average masses of 2352.8,

TABLE 1

Comparison of previously characterized conantokins with *C. parius* conantokins

Con, conantokin; γ, γ-carboxyglutamate; O, 4-*trans*-hydroxyproline; *, C-terminal amidation; ^, C-terminal free acid. Consensus sequences from previously characterized conantokins are underlined. Differences from the previous consensus in the newly characterized conantokins are in boldface type.

Conus Species	Conantokin	Amino-Acid Sequence	Ref.
C. geographus	Con-G	GE γγ LQ γ NQ γ LIR γ KSN*	(1)
C. lynceus	Con-L	GE γγ VA K MAA γ LAR γ DAVN*	(7)
C. radiatus	Con-R	GE γγ VA K MAA γ LAR γ NIAKGCKVNCYP^	(6)
C. tulipa	Con-T	GE γγ YQ K ML γ NLR γ AEVKKNA*	(3)
C. parius	Con-Pr1	GE **D**γ YA γ GIR γ YQ**L** **I** HGKI^	This work
C. parius	Con-Pr2	**DE** **O**γ YA γ AIR γ YQ**L** **K** YGKI^	This work
C. parius	Con-Pr3	GE **O**γ VA K WA γ GLR γ KAASN*	This work

TABLE 2

Nucleotides and predicted amino acids for conantokin sequences cloned from *C. parius* venom-duct cDNA

Conantokin	Nucleotide- and Predicted Amino-Acid Sequences
Con-Pr2	D E P E Y A E A I R E Y Q L K Y G K I GACGAACCCGAATATGCAGAAGCGATAAGAGAGTATCAACTTAAATATGGGAAAATA
Con-Pr3	G E P E V A K W A E G L R E K A A S N GGCGAACCAGAAGTTGCAAAATGGGCAGAGGGTCTAAGAGAAAAGGCAGCTTCAAAC

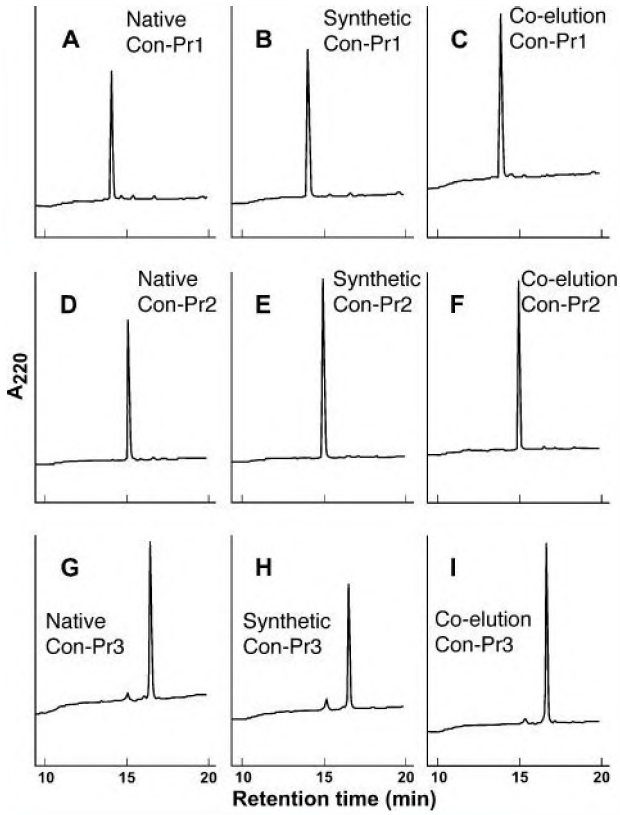

FIGURE 2. **HPLC co-elution of native and synthetic conantokins.** Elution was done with a gradient of 20–70% solvent B (0.085% trifluoroacetic acid in 90% acetonitrile) in each case. *A*, native con-Pr1; *B*, synthetic con-Pr1; *C*, native/synthetic con-Pr1; *D*, native con-Pr2; *E*, synthetic con-Pr2; *F*, native/synthetic con-Pr2; *G*, native con-Pr3; *H*, synthetic con-Pr3; *I*, native/synthetic con-Pr3.

2309.4, 2265.9, and 2222.2, indicating the decarboxylation of the three Gla residues, consistent with the calculated mass of 2352.4 of the intact peptide. The peptide was referred to as conantokin-Pr1 (con-Pr1).

TABLE 3

IC injections of 10-day-old Swiss-Webster mice

Peptide injected (or saline)	Dosage	No. of mice injected	No. of mice in sleep-like state	Average onset of deep sleep (Minutes)
	nmol			
Saline (−control)	NA[a]	4	0	NA
Con-G (+ control)	5	4	4	3.9
	1	4	4	10.0
	0.5	4	2	10.5
Con-Pr1	5	4	4	9.0
	1	6	5	12.2
	0.5	5	4	18.0
Con-Pr2	5	3	3	9.7
	1	2	2	14.0
	0.5	2	2	17.5
Con-Pr3	5	3	3	10.7
	1	2	2	16.5
	0.5	3	2	21.0

[a] NA means not applicable.

The purified peptide in Fig. 1*G* includes 19 amino acid residues and has the sequence DEOγYAγAIRγYQLKYGKI^ where *O* indicates 4-*trans*-hydroxyproline (Hyp). Based on MALDI mass spectrometry, the peptide has average masses of 2462.8, 2419.2, 2375.4, and 2331.3, in agreement with the calculated mass of 2463.6 of the intact peptide. The peptide was designated conantokin-Pr2 (con-Pr2).

Fig. 1*K* shows a homogeneous peak of the peptide containing 19 amino acid residues with the sequence GEOγVAKWAγGLRγKAASN*, where * indicates C-terminal amidation. The average masses determined by MALDI were 2189.6, 2146.2, 2102.7, and 2058.5 (calculated mass of the intact peptide = 2189.2). The peptide was named conantokin-Pr3 (con-Pr3).

The genes encoding two of these conantokins have been cloned, confirming the sequences and indicating that the peptides belong to the conantokin family (Tables 1 and 2). Each of the three peptide sequences isolated was unique and different

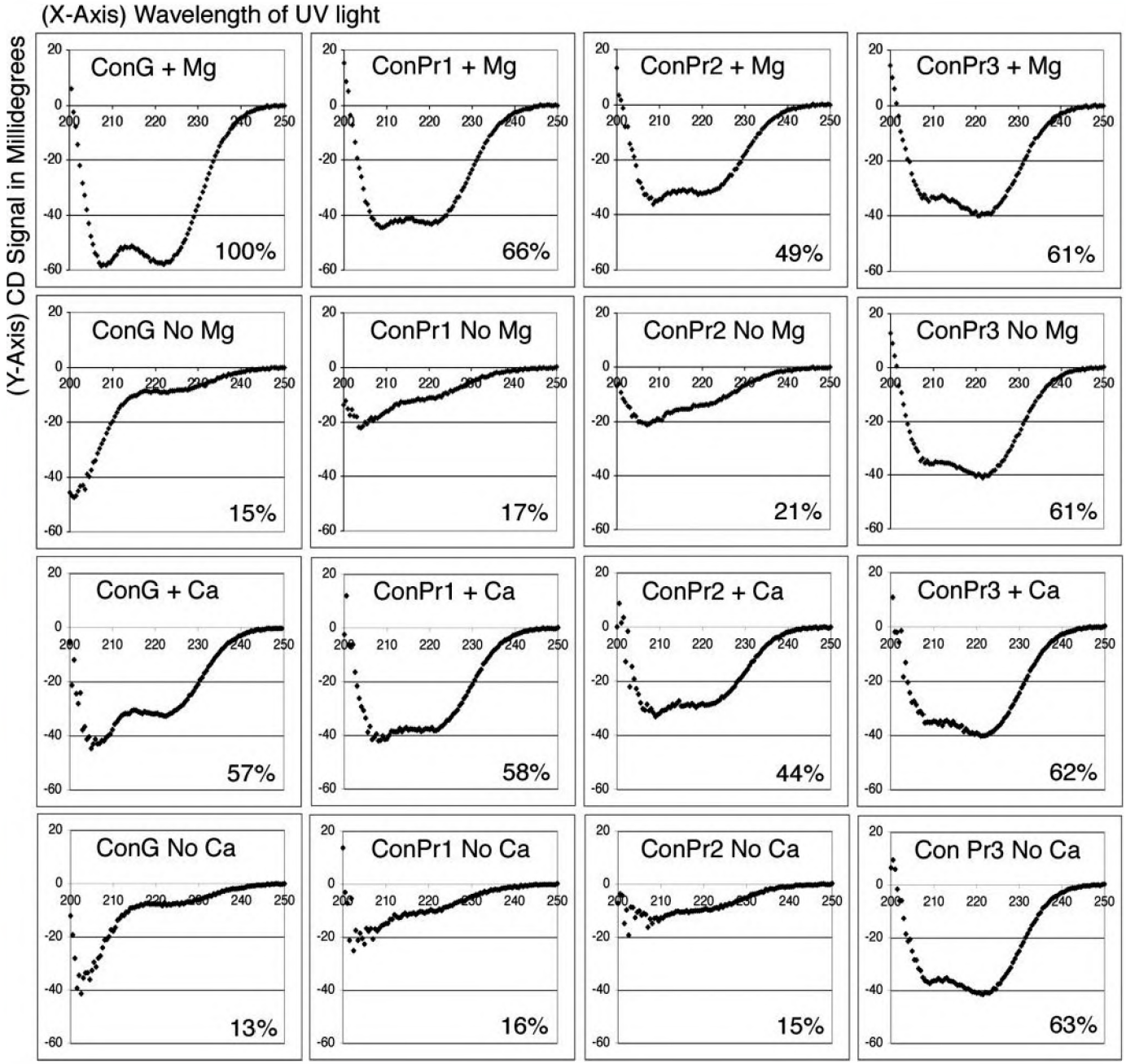

FIGURE 3. **Circular dichroism spectroscopy of *C. parius* conantokins and con-G.** In each case, the *x* axis is wavelength of UV light (200–250 nm), and the *y* axis is the CD signal in millidegrees. Dual minima at 208 and 222 nm are characteristic of α-helix. The % α-helix is shown in the *lower right corner* of each box and was estimated as described under "Experimental Procedures." The *top two rows* show the raw circular dichroism data for each peptide in 10 mM phosphate buffer, pH 7, either in the presence or absence of 2 mM $MgCl_2$. The *bottom two rows* show the raw circular dichroism data for each peptide in 10 mM HEPES buffer, pH 7, either in the presence or absence of 2 mM $CaCl_2$.

from all previously characterized conantokins. Thus, further in-depth characterization of these peptides was undertaken at this point.

Peptide Synthesis—Con-Pr1, -Pr2, and -Pr3 were synthesized on solid support as described under "Experimental Procedures." Mass spectrometry confirmed that native and synthetic peptides had the same masses. In each case, an HPLC fraction of synthetic peptide that eluted with the same retention time as the native peptide also co-eluted with the native peptide when equal quantities of native and synthetic peptide were co-injected into an HPLC column (Fig. 2). The peptide sequencing, molecular cloning, mass spectrometry, and HPLC co-elution data all indicate that the native and synthetic conantokin peptides are chemically identical.

In Vivo Biological Activities—All three conantokins (con-Pr1, -Pr2, and -Pr3) induced a sleep-like state in 10-day-old mice and hyperactivity (continuous walking, excessive grooming, and climbing of cage wall) in 24-day-old mice, characteristic of known conantokins (1, 3, 7). An initial screen of the venom-purified conantokins indicated that 1 nmol of each conantokin injected intracranially into 10-day-old mice (6.8–7.2 g) induced light sleep (easily awakened with a touch), which

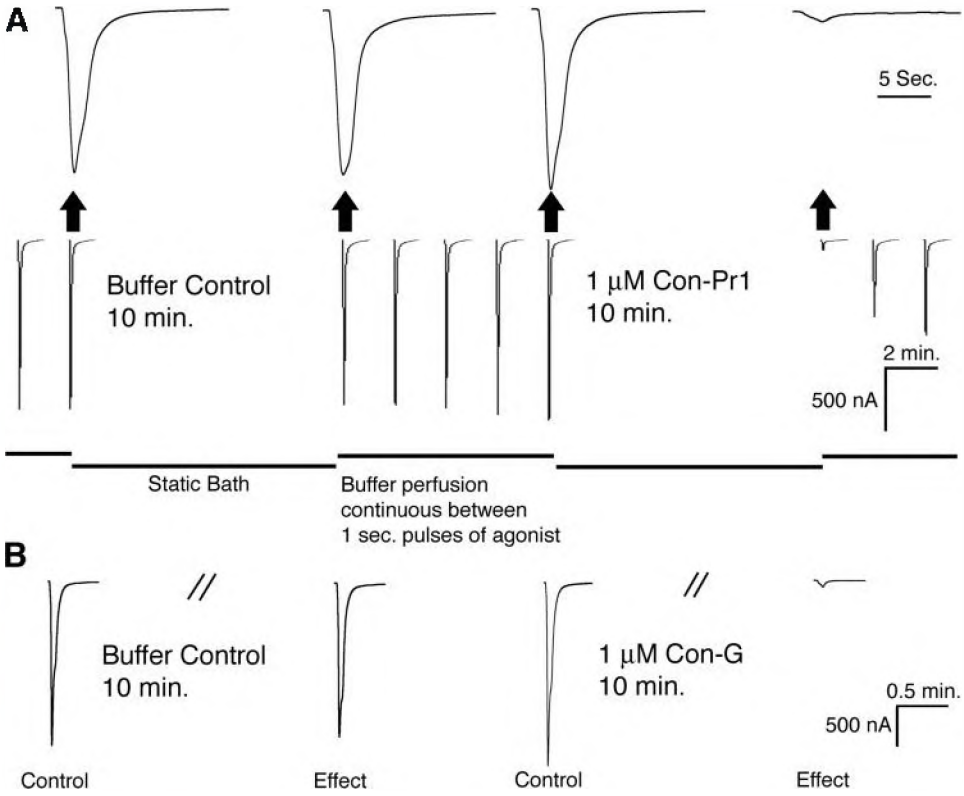

FIGURE 4. **Current traces from NR1–3b/NR2B NMDA receptors expressed in *Xenopus* oocytes.** Current traces in each panel were obtained sequentially (*left* to *right*) as described under "Experimental Procedures." *A*, two current traces were obtained to establish a base line for current amplitude, followed by a 10-min buffer control, during which no peptide was added to the bath, but buffer flow was halted (static bath). After agonist pulses and buffer perfusion resumed (*middle five current traces*), it was evident that the base-line current amplitude had not changed significantly. After establishing that control, 1 μM con-Pr1 was applied to the oocyte in a static bath for 10 min. The first agonist-elicited current trace following the application of con-Pr1 indicated that the elicited current was blocked nearly completely by the peptide, which began to dissociate from the receptor and wash out upon resumption of buffer perfusion (*final three current traces*). The current traces above the *arrows* show an expanded view of 15 s of each trace directly below the *arrow*, demonstrating the shape of each current trace. *B*, the same protocol as in *A* was followed, using con-G which served as a positive control for block of NR2B-containing NMDA receptors.

eventually progressed to deep sleep. The three conantokins initially appeared to be almost equally potent in inducing sleep with onset times of light sleep ~9–11 min after injection. Two nmol of each conantokin in 24-day-old mice (12.2–12.8 g) generally caused hyperactivity within ~5–8 min from injection time lasting for ~40 min. Native and synthetic peptides demonstrated the same biological activity, confirming that native and synthetic peptides are identical.

With the synthetic conantokins, we explored the induction of sleep in 10-day-old mice in more quantitative detail, utilizing con-G as a positive control. For this assay (see Table 3), the onset of deep sleep was defined as the time at which mice would no longer attempt to roll to their feet after being rolled onto their backs. Saline-injected negative controls always rolled to their feet immediately upon being rolled onto their backs. As demonstrated in Table 3, higher dosages of each conantokin induced sleep more rapidly than lower dosages. In general, the duration of sleep also appeared to be a function of conantokin dosage, with longer duration of sleep associated with higher dosages. However, it was difficult to quantify recovery time because in many cases, mice injected with 0.5–1.0 nmol of a conantokin would partially recover from their sleep but would eventually return to the deep-sleep state where they would not roll over or struggle upon being rolled onto their backs. We have not provided a quantitative assessment of the hyperactivity induced in older mice because the onset of hyperactivity was difficult to identify with precision, and the hyperactivity (continuous walking, excessive grooming and climbing of cage wall) tended to be interrupted by periods of sleep.

Circular Dichroism Spectroscopy—Because con-Pr1, -Pr2, and -Pr3 all shared common characteristics of conantokins, we hypothesized that they would be structurally related to con-G, which adopts an α-helical conformation in solution in the presence of divalent cations. However, it is nearly structureless in the absence of divalent cations (22). To estimate the α-helical content of the *C. parius* conantokins, circular dichroism spectroscopy was employed. The α-helical content of con-Pr1 and -Pr2 was estimated to be much greater in the presence of Mg^{2+} or Ca^{2+} than in the absence of divalent cations, like con-G (Fig. 3). The estimated α-helical content of con-G (as a control), con-Pr1, and con-Pr2 was greater in the presence of 2 mM Mg^{2+} than 2 mM Ca^{2+}, consistent with the previous observation that con-G has higher affinity for Mg^{2+} than Ca^{2+} and a more definitive structure in the presence of Mg^{2+} than Ca^{2+} (22). In contrast, con-Pr3 adopted a predominantly α-helical conformation in both the presence and absence of divalent cations (Fig. 3), similar to con-T (23).

Electrophysiology—Considering their sequence and structural similarity to other conantokins, which are known to inhibit NMDA receptors, we tested con-Pr1, -Pr2, and -Pr3 against rat NMDA receptors expressed in *Xenopus* oocytes. In each case, we expressed the NR1–3b splice variant with one NR2 subunit (A–D). Because con-G is reported to inhibit selectively NMDA receptors expressing the NR2B subunit, we used con-G as a control for our experiments.

To simulate synaptic neurotransmission, where high concentrations of neurotransmitter are released transiently and then rapidly cleared from the synaptic cleft, we employed the electrophysiological protocol described under "Experimental Procedures" for testing the conantokin peptides. As shown in Fig. 4, 1 μM concentration of con-Pr1 blocked most of the current elicited from voltage-clamped *Xenopus* oocytes expressing the rat NR1–3b/NR2B NMDA receptor, similar to con-G. Utilizing the same electrophysiological protocol employed in Fig. 4, concentration-response curves were generated for con-Pr1,

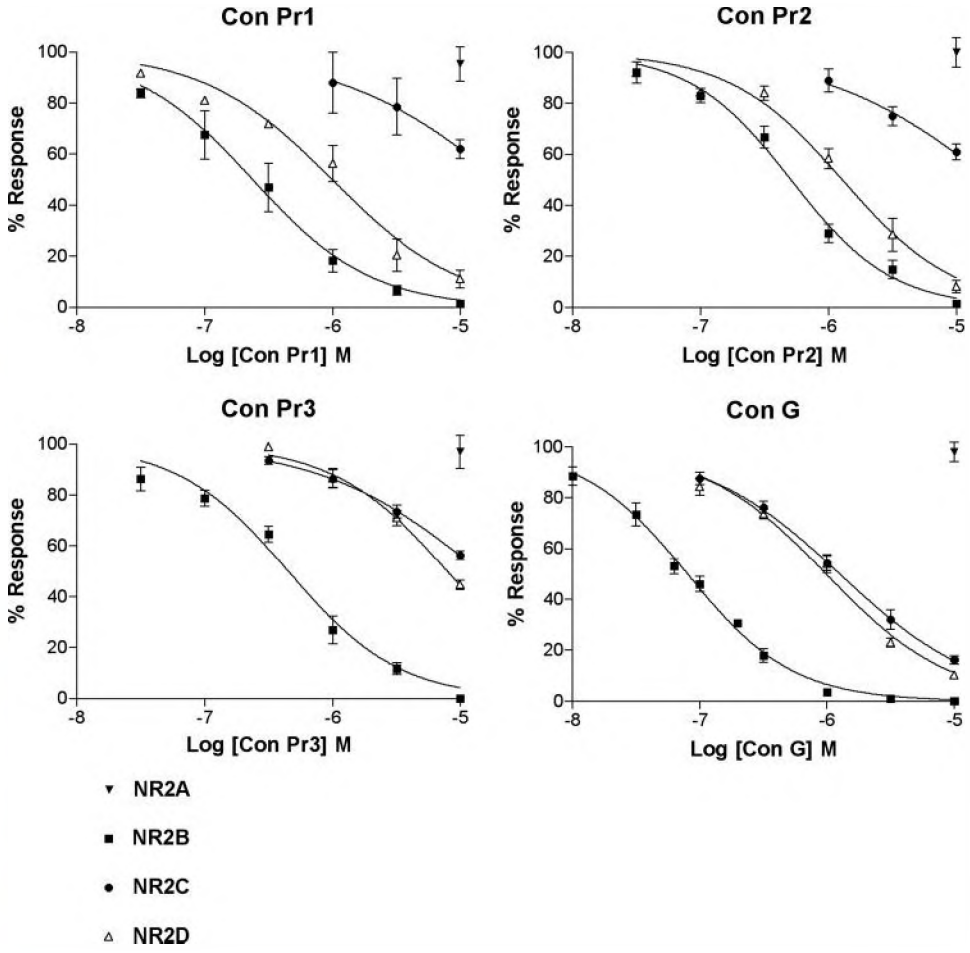

FIGURE 5. **Concentration-response curves for *C. parius* conantokins and con-G.** Various NMDA NR2 subunits were separately co-expressed with NR1–3b in *Xenopus* oocytes. The electrophysiology protocol described in Fig. 4 and under "Experimental Procedures" was employed to test various concentrations of each peptide against the different subunit combinations. Percent-response values and concentration-response curves were determined as described under "Experimental Procedures" ($n \geq 3$ tests for each data point).

TABLE 4

Approximate IC_{50} values for conantokins tested against various NR2 subunits

All data were obtained from the concentration-response curves in Fig. 5, with the exception of con-R data, which were obtained from White *et al.* (15).

Peptide	NR2A IC_{50}	NR2B IC_{50}	NR2C IC_{50}	NR2D IC_{50}	NR2D/NR2B IC_{50} ratio	NR2A/NR2D IC_{50} ratio
	μM	μM	μM	μM		
Con-Pr1	>>10	0.2	≥10	1	5	>>10
Con-Pr2	>>10	0.5	≥10	1	2	>>10
Con-Pr3	>>10	0.5	≥10	8	16	>10
Con-G	>>10	0.1	1	1	10	>>10
Con-R	1	1	7	>>10	>>10	<<0.1

-Pr2, -Pr3, and -G for all NR2 subunits in combination with the NR1–3b splice variant (Fig. 5). All of these conantokins inhibited the NR2B-subunit-containing receptors with highest relative potency (Fig. 5 and Table 4). Although con-Pr1 and -Pr2 also inhibited NR2D-containing receptors with relatively high potency, con-Pr3 demonstrated ~10-fold selectivity for NR2B, similar to con-G in our hands. To determine their selectivity for NMDA receptors, we tested each of these peptides against various ligand-gated ion channels. Based on this testing, each of the peptides appears to be specific for NMDA receptors. At 10 μM concentration, each peptide failed to inhibit, or minimally inhibited, currents elicited from nicotinic acetylcholine receptors or non-NMDA glutamate receptors (Fig. 6).

DISCUSSION

Previous discovery work on conantokins yielded a single peptide belonging to the conantokin family from each individual *Conus* venom examined. However, from the venom of *C. parius* three different conantokins were identified and characterized. This work has significantly expanded the number of conantokin peptides reported in the scientific literature and has contributed to our knowledge regarding conantokin structure-function relationships. The three newly discovered peptides, con-Pr1, -Pr2, and -Pr3, isolated from *C. parius*, reveal primary amino acid sequences with some general similarities to previously characterized conantokins (1, 3, 6, 7), most notably the presence of multiple Gla residues and the absence of disulfide bonds. However, these peptides vary from the previous conantokin consensus sequence at several positions (Table 1), suggesting that the conantokin family is more structurally and functionally diverse than previously thought.

In contrast to the previous conantokin consensus sequence, all of the *C. parius* peptides lack a Gla residue at the 3rd position from the N terminus; a residue of either Asp or Hyp is present at that position. Con-Pr1 and -Pr2 lack Arg and Gla residues at positions 13–14 or 14–15, whereas con-Pr2 has an N-terminal Asp rather than Gly. Furthermore, con-Pr3 is the first example of a conantokin containing three different post-translational modifications: γ-carboxyglutamate, 4-*trans*-hydroxyproline, and C-terminal amidation (Table 1). Because all conantokin peptides target NMDA receptors, the biochemical characteristics required for their functionality have been further elucidated by this work.

Conantokins are known for Ca^{2+}- and Mg^{2+}-induced conformational changes, where the divalent cations produce α-helical conformations from relatively unstructured peptides (24, 25). The α-helical content of con-Pr1 and -Pr2 increased substantially in the presence of physiologically relevant concentrations of divalent cations, similar to con-G (Fig. 3) (22). However, con-Pr3 is predominantly α-helical even in the absence of divalent cations (Fig. 3), similar to con-T (23). Con-G adopts an α-helical conformation along the entire length of the peptide in the presence of Mg^{2+} because the side chains of the Gla residues coordinate the divalent cations approximately along one

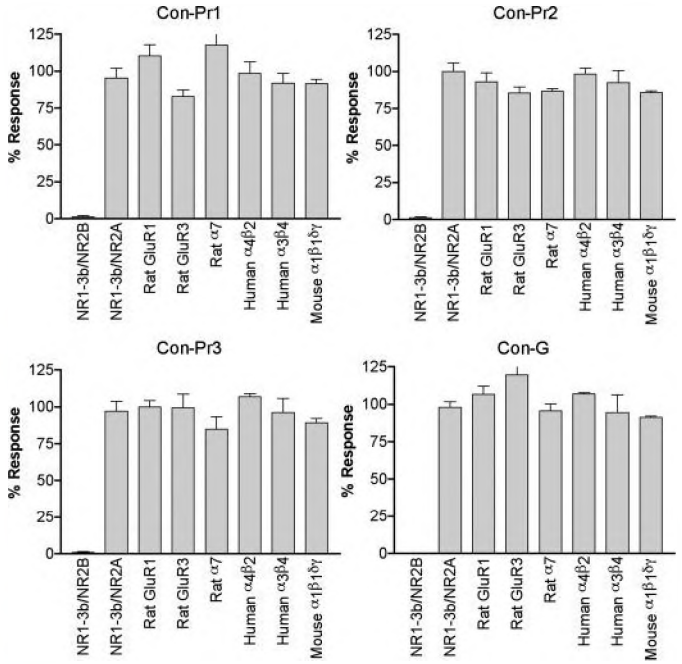

FIGURE 6. **Selectivity testing of *C. parius* conantokins and con-G against various ligand-gated ion channels.** In each case, 10 μM peptide was applied to oocytes expressing the various receptors as described under "Experimental Procedures." All conantokins blocked rat NR1–3b/NR2B NMDA receptors completely or nearly completely at 10 μM. However, these conantokins appeared to have little or no effect on other non-NMDA receptors tested. All the non-NMDA receptors tested are subtypes of nicotinic acetylcholine receptors, with the exceptions of GluR1 and GluR3, which are α-amino-3-hydroxy-5-methyl-4-isoxazole propionate-type glutamate receptors ($n \geq 3$ tests for each bar).

face of the α-helix. Substituting a different amino acid for any Gla residue decreased the α-helical content of con-G (22). Because con-G contains five Gla residues, whereas con-Pr1 and -Pr2 only have three Gla residues, the α-helical content of con-Pr1 and -Pr2 is less than the α-helical content of con-G in the presence of Mg^{2+} (Fig. 3).

The fact that con-Pr3 and con-T are substantially α-helical in the absence of divalent cations may be accounted for by the presence of a Lys residue at the 7th position from the N terminus, whereas con-G, -Pr1, and -Pr2 have a Gla residue at that position (Table 1). We hypothesize that the positively charged side chain of Lys stabilizes the α-helical conformation through favorable electrostatic interactions with the negatively charged side chains of Gla residues that align along the same face of the α-helix, most likely at positions 4 and 10 from the N terminus, significantly reducing the requirement of divalent cations for stabilizing the α-helical conformation. This hypothesis was previously suggested for con-T by other researchers who demonstrated that when Lys at position 7 was replaced by Gla, the peptide had low α-helical content in the absence of divalent cations. They proposed that Gla destabilizes the α-helix in the absence of divalent cations through electrostatic repulsion of the other negatively charged Gla side chains that would align with Gla at position 7 in an α-helical conformation (26).

Con-R also contains a Lys residue at the 7th position from the N terminus (Table 1). However, its structural relationship to the other conantokins is unique because it contains a disulfide bond near the C terminus. Although native con-R was estimated to be less than 35% α-helical, even in the presence of divalent cations, several C-terminal truncations of con-R increased the α-helical content of con-R in both the absence and presence of divalent cations. Some of the C-terminal truncations were estimated to be substantially α-helical in the absence of divalent cations, *e.g.* 45% α-helix for con-R residues 1–14 (27). This observation is consistent with the hypothesis that the Lys residue at position 7 stabilizes the α-helical conformation in conantokins that lack a disulfide bond in the absence of divalent cations. There are no structural data available for con-L, which also contains Lys at position 7.

Although con-T was found to be substantially α-helical in the absence of divalent cations (~50%), the presence of divalent cations increased the estimated α-helical content (~80%) (23–25). Therefore, it is particularly surprising that con-Pr3 appears to be ~60% α-helical in both the presence and absence of divalent cations (Fig. 3). One possible explanation for this apparent difference between peptides is the presence of Hyp at the 3rd position from the N terminus in con-Pr3, which may further stabilize the α-helical conformation in the absence of divalent cations, in conjunction with Lys at position 7.

Despite structural differences, the *C. parius* peptides are functionally similar to other conantokins, particularly con-G. Like con-G, all of the *C. parius* conantokins induce sleep in young mice and hyperactivity in older mice. Furthermore, they all inhibit NMDA receptors that contain an NR2B subunit with highest efficacy. In our hands, con-Pr3 exhibited selectivity for NR2B that is similar in magnitude to the selectivity of con-G. All of the *C. parius* conantokins, as well as con-G, appear to be specific for NMDA receptors, as they did not affect activity of other ligand-gated ion channels.

Con-Pr2 exhibited greater inhibition of NR2D, relative to NR2B, than previously characterized conantokins, as shown in Table 4. Although the basis for this lack of selectivity between NR2B and NR2D is unknown, there are several possibilities that may be explored in future studies. For example, con-Pr2 is the only known conantokin to contain Asp at the N terminus, which may play a role in the relatively higher potency for NR2D. However, con-Pr1 also appears to discriminate less between NR2B and NR2D than either con-Pr3 or con-G (Table 4). Among other similarities between con-Pr1 and -Pr2 (not shared by con-Pr3 or -G), they contain a Tyr at position 5 from the N terminus, which may also play a role in potency for NR2D relative to NR2B.

For the five peptides shown in Table 4, all peptides have a bias for NR2B. However, con-R is a more potent antagonist of NR2A than NR2D, as determined previously (15), and confirmed by us, using the same electrophysiological protocol employed in this work (data not shown). In contrast, the *C. parius* conantokins and con-G are more potent antagonists of NR2D than NR2A, as shown in Fig. 5 and Table 4. Cumulatively, these data provide a concrete basis for exploring the structural features in conantokin peptides that determine relative potency of block for NR2A *versus* NR2D.

The emerging structural diversity of conantokins is likely to reveal more functional diversity among conantokin peptides. Clearly, the characterization of more native conantokin pep-

tides should reveal additional structural determinants that are important for selectivity between NMDA receptor subtypes.

REFERENCES

1. McIntosh, J. M., Olivera, B. M., Cruz, L. J., and Gray, W. R. (1984) *J. Biol. Chem.* **259,** 14343–14346
2. Olivera, B. M., Cruz, L. J., and Yoskikami, D. (1999) *Curr. Opin. Neurobiol.* **9,** 772–777
3. Haack, J. A., Rivier, J., Parks, T. N., Mena, E. E., Cruz, L. J., and Olivera, B. M. (1990) *J. Biol. Chem.* **265,** 6025–6029
4. Hammerland, L. G., Olivera, B. M., and Yoshikami, D. (1992) *Eur. J. Pharmacol.* **226,** 239–244
5. Mena, E. E., Gullak, M. F., Pagnozzi, M. J., Richter, K. E., Rivier, J., Cruz, L. J., and Olivera, B. M. (1990) *Neurosci. Lett.* **118,** 241–244
6. White, H. S., McCabe, R. T., Abogadie, F., Torres, J., Rivier, J. E., Paarmann, I., Hollmann, M., Olivera, B. M., and Cruz, L. J. (1997) *Soc. Neurosci. Abst.* **23,** 2164
7. Jimenez, E. C., Donevan, S. D., Walker, C., Zhou, L.-M., Nielsen, J., Cruz, L. J., Armstrong, H., White, H. S., and Olivera, B. M. (2002) *Epilepsy Res.* **51,** 73–80
8. Donevan, S. D., and McCabe, R. T. (2000) *Mol. Pharmacol.* **58,** 614–623
9. Heading, C. E. (2002) *Curr. Opin. Investig. Drugs* **3,** 915–920
10. Williams, A. J., Dave, J. R., Phillips, J. B., Lin, Y., McCabe, R. T., and Tortella, F. C. (2000) *J. Pharmacol. Exp. Ther.* **294,** 378–386
11. Williams, A. J., Ling, G., McCabe, R. T., and Tortella, F. C. (2002) *Neuroreport* **13,** 821–824
12. Bleakman, D., Alt, A., and Nisenbaum, E. S. (2006) *Semin. Cell Dev. Biol.* **17,** 592–604
13. Layer, R. T., Wagstaff, J. D., and White, H. S. (2004) *Curr. Med. Chem.* **11,** 3073–3084
14. Malmberg, A. B., Gilbert, H., McCabe, R. T., and Basbaum, A. I. (2003) *Pain* **101,** 101–116
15. White, H. S., McCabe, R. T., Armstrong, H., Donevan, S., Cruz, L. J., Abogadie, F. C., Torres, J., Rivier, J. E., Paarman, I., Hollmann, M., and Olivera, B. M. (2000) *J. Pharmacol. Exp. Ther.* **292,** 425–432
16. Wei, J., Dong, M., Xiao, C., Jiang, F., Castellino, F. J., Prorok, M., and Dai, Q. (2006) *Neurosci. Lett.* **405,** 137–141
17. Cruz, L. J., Corpuz, G., and Olivera, B. M. (1976) *Veliger* **18,** 302–308
18. Edman, P., and Begg, G. (1967) *Eur. J. Biochem.* **1,** 80–91
19. Jacobsen, R., Jimenez, E. C., Grilley, M., Watkins, M., Hillyard, D., Cruz, L. J., and Olivera, B. M. (1998) *J. Pept. Res.* **51,** 173–179
20. Clark, C., Olivera, B. M., and Cruz, L. J. (1981) *Toxicon* **19,** 691–699
21. Cartier, G. E., Yoshikami, D., Gray, W. R., Luo, S., Olivera, B. M., and McIntosh, J. M. (1996) *J. Biol. Chem.* **271,** 7522–7528
22. Chen, Z., Blandl, T., Prorok, M., Warder, S. E., Li, L., Zhu, Y., Pedersen, L. G., Ni, F., and Castellino, F. J. (1998) *J. Biol. Chem.* **273,** 16248–16258
23. Prorok, M., Warder, S. E., Blandl, T., and Castellino, F. J. (1996) *Biochemistry* **35,** 16528–16534
24. Prorok, M., and Castellino, F. J. (2001) *Curr. Drug Targets* **2,** 313–322
25. Prorok, M., and Castellino, F. J. (2007) *Curr. Drug Targets* **8,** 633–642
26. Blandl, T., Warder, S. E., Prorok, M., and Castellino, F. J. (1999) *J. Pept. Res.* **53,** 453–464
27. Blandl, T., Zajicek, J., Prorok, M., and Castellino, F. J. (2001) *J. Biol. Chem.* **276,** 7391–7396